A self-purifying microfluidic system for identifying drugs acting against adult schistosomes

Vincent Girod, Robin Houssier, Karin Sahmer, Marie-José Ghoris, Stéphanie Caby, Oleg Melnyk, Colette Dissous, Vincent Senez, Jérôme Vicogne

ROYAL SOCIETY OPEN SCIENCE

royalsocietypublishing.org/journal/rsos

Research

Cite this article: Girod V, Houssier R, Sahmer K, Ghoris M-J, Caby S, Melnyk O, Dissous C, Senez V, Vicogne J. 2022 A self-purifying microfluidic system for identifying drugs acting against adult schistosomes. *R. Soc. Open Sci.* **9**: 220648. https://doi.org/10.1098/rsos.220648

Received: 27 May 2022
Accepted: 9 November 2022

Subject Category:
Engineering

Subject Areas:
microsystems/health and disease and epidemiology

Keywords:
schistosomiasis, microfluids, parasite, whole worms, drug screening, media optimization

Authors for correspondence:
Vincent Senez
e-mail: vincent.senez@univ-lille.fr
Jérôme Vicogne
e-mail: jerome.vicogne@ibl.cnrs.fr

†Both authors contributed equally to the work.

Electronic supplementary material is available online at https://doi.org/10.6084/m9.figshare.c.6306035.

THE ROYAL SOCIETY PUBLISHING

A self-purifying microfluidic system for identifying drugs acting against adult schistosomes

Vincent Girod[1,2,3,4], Robin Houssier[1,3], Karin Sahmer[5], Marie-José Ghoris[3], Stéphanie Caby[3], Oleg Melnyk[3], Colette Dissous[3], Vincent Senez[1,2,†] and Jérôme Vicogne[3,†]

[1]University of Lille, CNRS, Inserm, CHU Lille, UMR9020-U1277 – CANTHER – Cancer Heterogeneity Plasticity and Resistance to Therapies, Lille F-59000, France
[2]CNRS, University of Tokyo, IRL2820 – LIMMS, Lille F-59000, France
[3]University of Lille, CNRS, Inserm, CHU Lille, Institut Pasteur de Lille, U1019-UMR9017 – CIIL – Center for Infection and Immunity of Lille, F-59000 Lille, France
[4]University of Lille, CNRS, UPHF, JUNIA, CLI, UMR 8520 – IEMN – Institut d'Electronique, de Microélectronique et de Nanotechnologie, Villeneuve d'Ascq F-59650, France
[5]University of Lille, IMT Lille Douai, University of Artois, JUNIA, ULR 4515 – LGCgE, Laboratoire de Génie Civil et géo-Environnement, F-59000 Lille, France

JV, 0000-0001-8360-7497

The discovery of novel antihelmintic molecules to combat the development and spread of schistosomiasis, a disease caused by several *Schistosoma* flatworm species, mobilizes significant research efforts worldwide. With a limited number of biochemical assays for measuring the viability of adult worms, the antischistosomicidal activity of molecules is usually evaluated by a microscopic observation of worm mobility and/or integrity upon drug exposure. Even if these phenotypical assays enable multiple parameters analysis, they are often conducted during several days and need to be associated with image-based analysis to minimized subjectivity. We describe here a self-purifying microfluidic system enabling the selection of healthy adult worms and the identification of molecules acting instantly on the parasite. The worms are assayed in a dynamic environment that eliminates unhealthy worms that cannot attach firmly to the chip walls prior to being exposed to the drug. The detachment of the worms is also used as second step readout for identifying active compounds. We have validated this new fluidic screening approach using the two major antihelmintic drugs, praziquantel and artemisinin. The reported dynamic system is

simple to produce and to parallelize. Importantly, it enables a quick and sensitive detection of antischistosomal compounds in no more than one hour.

1. Introduction

Schistosomiasis is caused by flatworms of the genus *Schistosoma* and is the second most important parasitic disease, infecting more than 240 million people worldwide [1,2]. An outbreak of schistosomiasis in Corsica (France) since 2013 raises fears of an expansion of this parasitosis in southern Europe in the coming decades [3]. The pathology of schistosomiasis is due to the reaction of the host to schistosome eggs that accumulate in tissues during their intense and permanent production by adult worm couples, a problem worsened by their remarkable longevity (several decades). In the mammal host, mature male and female worms are paired and reside in blood vessels in a final location that varies according to the schistosome species. Adult couples of *Schistosoma mansoni*, the species that shows the widest geographical distribution and is used in this study, locate to the mesenteric veins (figure 1*a*) [4].

Since there is a real difficulty in developing a vaccine against schistosomiasis [5], the therapeutic treatment of the disease is still achieved by oral administration of praziquantel (PZQ) [6]. PZQ has a strong lethal effect against adult worms. Unfortunately, it is significantly less active against the juvenile forms that penetrated the skin, i.e. the schistosomula. Therefore, the treatment must be repeated regularly [7]. In addition, as PZQ has been used extensively in infected countries for many years, the development of tolerant parasite strains is now observed [8]. Specifically, lower efficacy has been demonstrated both in the laboratory and the field [9–11]. Therefore, there is now an urgent need to introduce new anti-schistosome treatments.

Schistosoma mansoni schistosomula, the juvenile form of the parasite, can be produced in high numbers using fresh cercariae released from its intermediate host, the snail *Biomphalaria glabrata*. However, besides very recent improvements of culture media composition favouring *in vitro* worm maturation from juveniles [12], adult worm couples have to be collected by blood perfusion from the mammal host, usually a rodent (mouse or hamster), and are assayed subsequently.

Different approaches to evaluate compounds against juvenile or mature worms have been developed [13]. The most advanced assays have been devised for the analysis of schistosomula. These assays use and sometimes combine image-based analysis allowing high-content screening [14,15], metabolic [16,17] and electro-impedance techniques [18,19]. Importantly, several of them can be automated and are able to assay a large number of juvenile worms for high-throughput screening (HTS), generating more relevant data, although they give no information about the efficacy of the compounds on the adult stage.

Comparatively, the assays analysing the response of adult worms to drugs are less diversified. However, over the last decades significant advances have been made in the development of medium-throughput screening and HTS systems [20]. These systems are based on sophisticated image- [21] or non-image-based systems combining biophysical parameters such as electrical impedance [22] or heat flow [23]. However, their design necessarily enables testing of a more limited number of adult worms (1–5 pairs) per assay compared with those analysing schistosomula (up to 1000). Complementary, several biochemical assays are also available to evaluate the viability of adult worms. These assays measure the metabolic activity of worms by quantifying ATP production [17], oxidative potential [24] or apoptotic stress that can be also imaged (Fast Blue BB [25], TUNEL [26]). One of the most advanced biochemical assays quantifies lactate production by juvenile and adult worms and allows a precise assessment of worm viability in larger population but also the selection of single healthy worm prior to phenotypic and genetic analysis [27,28].

However, phenotypic analysis of whole worms *in vitro* still remains the most widely used approach to identify active compounds for adult worms [29,30]. Despite the development of automated motion-based systems such as WormAssay [31], these analyses are usually done by a visual scoring of morphological and/or behavioural changes, mostly centred on motility parameters (figure 1*b*) [32]. A numerical scale called the 'severity score' [33], usually comprising four [17] or five [34] score levels, is used to describe deleterious phenotypes. Although these scoring methods have been shown to be effective in identifying drug candidates that later showed efficacy in a mouse model of *S. mansoni* infection [35], they are difficult to set up and parallelize when based on a manual assessment. Moreover, the limited and inconstant viability of the worms *ex vivo* can affect the reproducibility and reliability of these assays. Above all, most of *in vitro* assays do not allow measurement of the sole effect of a drug while

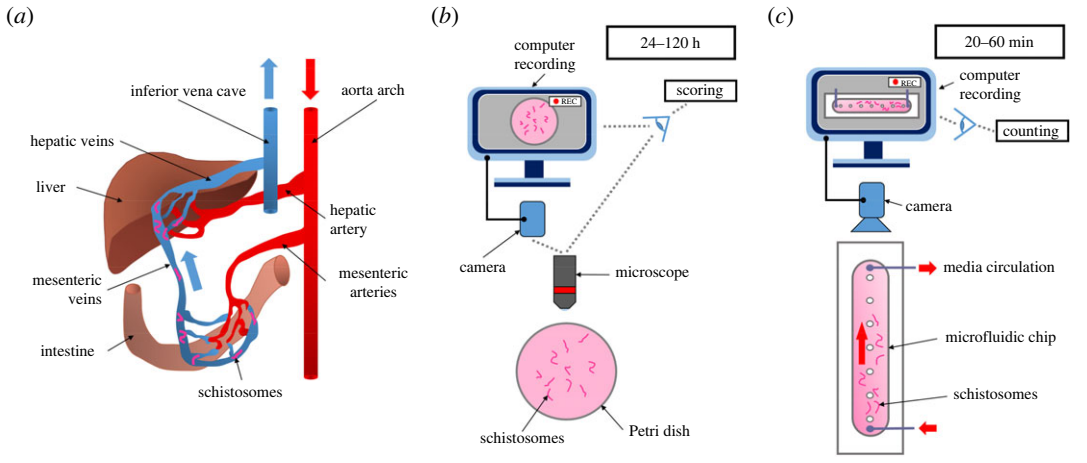

Figure 1. Physiological localization of schistosomes in vertebrate hosts and comparison of static and dynamic drug characterization studies. (*a*) In their mammal hosts, adult schistosomes are localized in the mesenteric veins with bloodstream oriented from intestine towards the liver. (*b*) During *in vitro* studies, worms are cultivated in static conditions in Petri dishes and observed under the microscope for 24–120 h to analyse phenotypes and survival rates. (*c*) In the dynamic system reported here, worms are introduced in a microfluidic chip with an oriented flow that force them to grip to the wall surface. Worm number is determined for 20–60 min after the introduction of the drug.

the diminution of the viability of the worms increases over time, a problem that is worsened by the duration of some phenotypic assays that are run for several days.

We therefore searched for a novel assay that would (i) furnish a quantitative response to a drug within a few hours and not days, (ii) be self-purifying by enabling the elimination of dying or weak worms before applying the drug, and (iii) be cost-effective together with a significant number of worms analysed per conditions.

We reasoned that assaying the worms under flow conditions might provide a new strategy using well-defined physical parameters to identify fast-acting drugs. Indeed, within infected hosts, healthy worms continuously grip the wall of the veins to resist the blood flow. Depending on vessel flow, viscosity and geometrical constraints, adult worms either use their oral and ventral suckers or favour a crawling mode of locomotion [36]. A worm with compromised viability quickly loses its ability to grip to the surface with its suckers and thus to maintain its position against the flow. Therefore, the adhesion of worms under flow conditions might not only offer a simple and efficient means for selecting the worms before starting the biological assay, it might also provide a quantitative and binary readout for measuring the effect of a drug (figure 1*c*).

In this work, we designed a single-channel microfluidic chip able to host 30 males, females or couples. We have evaluated different surface coatings for their effect on promoting worm adhesion and motility under flow conditions. Having achieved the conditions for enabling the worms to strongly grip the chip walls by oral and ventral suckers, we used the chip to select healthy worms and probe their resistance against the flow to increasing doses of PZQ or artemisinin (ART).

2. Materials and methods

2.1. Parasite material

All animal experimentations were conducted in accordance with the European Convention for the Protection of Vertebrate Animals used for Experimental and other Scientific Purposes (ETS no. 123, revised Appendix A) and were approved by the local committee for ethics in animal experimentation (authorization no. APAFIS#8289-2016122015127050v3) and the Pasteur Institute of Lille (agreement no. B59350009).

A Puerto Rican strain of *S. mansoni* is maintained in the laboratory using the intermediate snail host *Biomphalaria glabrata* and the definitive golden hamster host *Mesocricetus auratus*. *Schistosoma mansoni* adult worms were obtained by hepatic portal perfusion of hamsters, six weeks after having been infected by cercariae released from infected snails [37]. Perfused worms were immediately washed with RPMI culture medium (RPMI 1640 GIBCO, 61870-010, UK), transferred into fresh RPMI culture medium

supplemented with heat-inactivated horse serum (10%, GIBCO, 16050-122, UK), rifampicin (60 µg mL^{-1}, EUROMEDEX, 1059, Souffelweyersheim, France), penicillin (50 units mL^{-1}) and streptomycin (50 µg mL^{-1}, SIGMA, P-4333, USA).

2.2. Worm culture medium optimization and viability in various media and sera

Typically, immediately after perfusion, 100–150 worms were incubated in 100 mm Petri dish plates containing 25 mL of complete RPMI medium for 2–3 h in order to allow separated male and female worms to pair again (37°C, saturated humid atmosphere, 5% CO_2). Worms were maintained for a maximum of 5 days after perfusion and culture medium was renewed every 12 h. For medium testing experiments, 10 couples were maintained up to one month in six-well plates (9.6 cm^2) using 3 mL of M199 (GIBCO, 41150-020, UK), DMEM (GIBCO, 61965-026, UK) or RPMI supplemented either with 10% of heat-inactivated fetal calf serum (PAA, A15-101, AT), horse serum or human serum (Institute Pasteur of Lille, France). All medium/serum combinations were supplemented with antibiotics, as described above and 2 mL of medium were exchanged with fresh medium every 48 h. The experiment was repeated eight times ($n = 8$). The viability of the worms was evaluated by observing the parasites with a macroscope (OPTIKA, SZ6745TR, Italy) and using a visual 'severity score' to determine health status [20,38,39]. We have defined a three-level scale: S2 score is for worms having a normal movement, gut peristalsis and normal tissues and tegument integrity, are attachment to plate with sucker, S1 score corresponds to worms with reduced movement but still gut peristalsis and/or degraded tissues or tegument, while S0 corresponds to dead worms having no movement or with strong tissue degradation. Each condition was observed for at least 30 s. Data were corrected when an S0 score (dead) was followed by an S1 or S2 score (still alive) and thus to avoid falsely counting worms that were still alive as dead. The data are presented as percentages, mean values and standard deviations. Statistical significance was calculated with ANOVA followed by Tukey's test with an alpha risk of 5% (p-value < 0.05) between human, calf and horse sera. Assumptions of ANOVA were verified by using a plot of residuals in function of predictions and a normal qq-plot. All these data analysis were done using R Software [] under RStudio environment (1.1.463 release, RStudio Inc., Boston, USA)

2.3. Madin-Darby canine kidney cell culture

Madin-Darby canine kidney cells (MDCK, ATCC, USA, p11, 2008) were cultured in DMEM medium supplemented with 10% of heat-inactivated fetal bovine serum (GIBCO, 10270-106, USA), 1% (v/v) of non-essential amino acids (GIBCO, 11140-050, USA), biotin (50 µg mL^{-1}, SIGMA, B4639, USA) and ZellSchield® 1X (ZellSchield®, 13-0150, Germany), called MDCK medium. At subconfluence, cells were seeded as advised according to the ATCC protocol.

2.4. Microfluidic chip design

The geometrical features of the chips were designed by using COMSOL Multiphysics (Comsol AB, Stockholm, Sweden) to obtain a single-microfluidic chamber; the fluid flow was calculated with the microfluidic module using laminar flow conditions assuming a very low Reynolds number (see electronic supplementary material, table S3). The three-dimensional finite element method (FEM) model is made of about 2 106 192 degrees of freedom using the predefined 'extra-fine' mesh refinement. In the fluid flow model, non-slip initial condition was imposed to all surfaces corresponding to a solid/liquid interface. A fixed flow rate (between 0.05 and 3.4 mL min^{-1}) was used for the inlet and a fixed pressure ($p = 0$ Pa) for the outlet. The equations were solved in 900 s requiring 7.5 Go using an Intel Core i7–7500 U CPU cadenced at 2.7 Ghz with 16 Go RAM configuration.

2.5. Microfluidic chip fabrication

The mould was fabricated on an aluminium substrate using a computer numerical control machine (MECANUMERIC, Charlyrobot DMC300, Marssac-sur-Tarn, France) to obtain 400 µm of height. A 2 µm layer of Parylene type C was deposited [41] using an evaporator (SCS LABCOTER, Indianapolis, PDS 2010, USA) to suppress milling surface defects and to favour polydimethylsiloxane (PDMS) (SYLGARD®, 184 Silicon Elastomer Kit, Dow Corning, Midland, USA) pilling. PDMS was fabricated using a standard process with a 10 : 1 elastomer base-curing agent ratio (w/w). The mixture was degassed and poured onto the mould up to approximately 5 mm thickness. The sample was

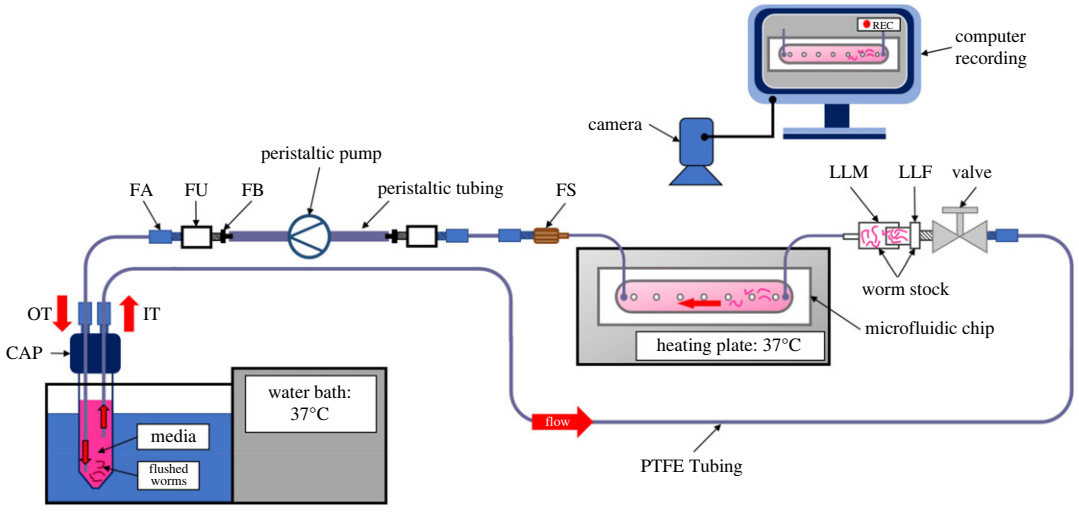

Figure 2. Schematic representation of the microfluidic experimental set-up. The culture medium supplemented or not with PZQ or ART was maintained at 37°C using a water bath and pulled with a peristaltic pump into the microfluidic chip at 1 mL min^{-1}. Chips were placed on a heating plate. The detachment of the worms in the microfluidic chip was video-recorded for 1 h. Components of the microfluidic network are described in the electronic supplementary material, figure S1.

cured at 95°C for 1 h. The PDMS channel layer was punched (1.5 mm outer diameter (OD), KAI Medical, Japan) to create media input and output ports (Inlet and Outlet respectively), cleaned with isopropanol and dried overnight. The PDMS was subsequently activated with air plasma and bound to a glass microscope slide to seal the channels. The chips were equipped with silicon tubing 0.5 inner diameter (ID) (IBIDI, 10840, Gräfelfing, Germany) and proper sealing was confirmed after perfusion with water.

2.6. Microfluidic network

Figure 2 gives a schematic representation of the experimental set-up (see electronic supplementary material for pictures of the full set-up, electronic supplementary material, figure S1). This network is made up of a Falcon tube (15 mL) with a microfluidic adapter (CAP) (DARWIN microfluidics, LVF-KPT-S-4, Paris, France) equipped with two plugs 1/4–28 (DARWIN microfluidics, CIL-P-309, Paris, France). These two plugs connect the inlet (IT) and outlet (OT) tubings to the remainder of the network. Both PTFE 1/32 ID tubings (DARWIN microfluidics, LVF-KTU-15, Paris, France) are equipped on both ends with 1/4–28 fitting associated with ferrules 1/16 OD (DARWIN microfluidics, LVF-KFI-06, Paris, France) (FA). IT is 45 cm long while OT is 50 cm long. Importantly, to prevent flushed worms being recaptured into the system, OT is totally immersed down to the very bottom of (approx. 10 cm) of the medium reservoir whereas IT is immersed by only 7.5 cm. IT is connected through FA to a shut-off valve (DARWIN microfluidics, LVF-KMM-08, Paris, France) (Valve). Worms are introduced into the circuit through a connector (Worm stock) composed of a Luer Lock Male (LLM) connector (IBIDI, 10826, Gräfelfing, Germany) and a Luer Lock Female (LLF) adapter 1/4–28 (DARWIN microfluidics, CIL-P-618, Paris, France). Silicone tubing 0.5 mm ID (IBIDI, 10841, Gräfelfing, Germany) connects the worm stock connector to the chip inlet as well as the chip outlet to the peristaltic pump (ISMATEC, IPC-N8 ISM936 Wertheim, Germany). A fitting 6–40 to 1/4–28 (DARWIN microfluidics, LVF-KFI-08, Paris, France) (FS) associated with FA connects the silicon tube to a PTFE tube (40 cm long). Connection to the pump is obtained through the association of FA with a 1/4–28 union (DARWIN microfluidics, LVF-KFI-10, Paris, France) (FU) and a 1/4–28 to 3/32 fitting (DARWIN microfluidics, LVF-KFI-06, Paris, France) (FB). The peristaltic pump tubing is 1.6 mm ID (ISMATEC, SC0425, Wertheim, Germany). Connection of the outlet of the pump to the PTFE 1/32 ID tubing OT is made with a FB + FU + FA association.

2.7. Device surface coating

Chip chambers were coated with 250 µg mL^{-1} of Type I-A collagen (FUJIFILM, Cellmatrix Type I-A, 631-00651, Neuss, Germany) solubilized in aqueous acetic acid (0.02 M) and introduced with a 1 mL syringe into the chip. After incubating at room temperature for 3 h, the chips were rinsed twice with 3 mL of

water. Chips were then connected to tubings and primed with 10 mL of complete RPMI medium prior to the connection of IT to CAP. For chips coated with MDCK cells, the inlet port was disconnected from tubing to introduce the MDCK cells (10.000 cells/chip) with a 1 mL syringe, then reconnected to the tubing. Finally, the circuit was connected to a peristaltic pump (ISMATEC, IPC-N8 ISM936, Wertheim, Germany) without flow for 3 h. Unattached cells were then flushed at 35 µL min^{-1} for 48 h, after which the 15 mL stock tube was replaced with a new one containing 9 mL of dedicated medium. After 48–72 h, MDCK cells reach full confluency.

2.8. Worm introduction into device

After having conditioned the microfluidic system, the peristaltic pump was stopped. The valve was closed and the circuit opened at the worm stock connector (disconnection between LLM and LLF). A 1 mL pipette tip was shortened approximately by 0.5 cm and used with a pipette to collect 30 couples and introduce them into LLM. To prevent bubble introduction into the circuit, LLM and LLF were filled by pipetting media before reconnection. The valve was opened again and the microfluidic chip connected to the peristaltic pump (ISMATEC, IPC-N8 ISM936, Wertheim, Germany). The pump was set for pulling the culture media at a flow rate of 75 µL min^{-1} and placed with the chip in an incubator to reduce tubing length and temperature drift (37°C, humid atmosphere, 5% CO_2). The system was primed for 30 min before starting the worm adhesion assay. Importantly, to avoid worms clogging the tubing and to disperse the worms within the chip, the system was placed vertically to let the couples settle by gravity. For that, the worm stock and microfluidic output were placed upwards and the microfluidic input placed downwards, as shown in electronic supplementary material, figure S2.

2.9. Adhesion studies on different surfaces

For each experiment, 30 couples were introduced into the chips with different glass surface coatings: w/o coating, coated with MDCK cells, with type I-A collagen or with both MDCK cells and type I-A collagen. Chips were placed on a heating block set at 37°C (Major Science, MD-02D, USA) and connected to 15 mL tubes placed in a water bath set at 37°C as depicted in figure 2. A camera (Microsoft, Q2F-00015, USA) was used to monitor the microfluidic channel at the beginning of the experiment in order to identify worms that lost adherence and to measure the duration of their residence in the microsystem before being flushed out by the flow. To modulate flow conditions, the peristaltic pump was programmed to pull the culture medium at different flow rates: (i) 50 to 300 µL min^{-1} with a step of 50 µL min^{-1} every min; (ii) 300 µL min^{-1} to 1 mL min^{-1} with a step of 100 µL min^{-1} every 2 min; and (iii) 1 to 3.4 mL min^{-1} with a step of 200 µL min^{-1} every 3 min. The percentages of worms still attached to the chip were plotted against the flow rate. A two-segment linear regression analysis was performed using SigmaPlot v. 14.5 with Piecewise fitting curve option to identify the transition value (T1, see electronic supplementary material, table S1). We next performed a linear regression using the data between 0 and 1.6 mL min^{-1} for glass, MDCK and collagen + MDCK, while the data between 500 µL min^{-1} and 1.6 mL min^{-1} values were used for collagen. This analysis furnished the slope of the first segments, the standard deviation and the 95% confidence intervals (see electronic supplementary material, table S2). Experiments were performed in duplicate ($n = 2$) with worms from the same age after perfusion and a 48 h maximum duration of culture. To compare gripping between males, females or couples, 30 worms or couples were introduced in a collagen-coated chip and were perfused at increasing flow rates as described above. Experiments were performed in triplicate ($n = 3$). Statistical significance was calculated with ANOVA followed by Tukey's test with an alpha risk of 5% (p-value < 0.05) between males, females and/or couples. The assumption of ANOVA was verified by using a plot of residuals in function of predictions and a normal qq-plot (see source data files).

2.10. Drug testing under flow conditions

PZQ (SIGMA, P-4668, USA) was prepared as a 0.5 M stock solution in DMSO and diluted in RPMI from 900 to 25 nM. ART (Tokyo chemical industry, A2118, Japan) was prepared as a 0.1 M stock solution in DMSO and diluted from 900 to 12.5 µM in RPMI. Stock solutions were stored at 4°C. Once the worms were introduced in the system as previously described, the flow rate was increased up to 1 mL min^{-1} by 200 µL min^{-1} increments every 5 s in order to favour worm attachment to the collagen-coated chips. The recording was started, and the 1 mL min^{-1} flow was maintained for 5 min. This lag period allowed the elimination of weakened worms. Next, PZQ or ART was added to the tube containing the culture

medium. The medium was mixed and infused into the device. The video recordings were used to count the worm couples present in the microfluidic chamber as a function of time. Experiments were performed in triplicate ($n = 3$) with worms from the same age after perfusion and with a maximum duration of culture prior experiment of 48 h.

2.11. Drug testing under static conditions

Typically, 10 worm couples were incubated in 12-well plates at 37°C for 120 h in RPMI supplemented with PZQ or ART (0 to 900 nM for PZQ or 0 to 900 µM for ART, 3 mL per well). The media were removed and renewed every 24 h. After this step, each well was immediately recorded for 15 s under a macroscope (OPTIKA, SZ6745TR, Italy) equipped with a camera (Microsoft, Q2F-00015, USA). In this experiment, we used a more resolved 'severity score' than those classically used for drug evaluation against helminths in static conditions [35]. We designed for this assay a five-level scoring since it gives a more precise evaluation of phenotypes, in particular paralysis or tegument alterations (S4 = normal mobility and blood sucker adhesion; S3 = reduction of mobility and/or loss of blood sucker adhesion; S2 = minimal mobility or occasional movements; S1 = no mobility except intestinal movement; S0 = total loss of mobility, no movement, death). Experiments were performed at least in triplicate for each concentration ($n > 3$) with freshly perfused worms (less than 12 h).

3. Results

3.1. Chip design

In order to generate a chip with a dynamic flow that forces worms to attach to the walls, we chose a simple design based on a single channel that can host a sufficient number of worms (30–40 couples) to improve the statistical significance of analysis. The chip had to be small enough to accommodate regular cameras and microscopes and to be parallelized. Thus, we designed a 1×5.8 cm single channel supported by seven pillars to prevent any sagging of the chip (figure 3*a*). In order to ease the elimination of the worms by the flow stream during treatments, we chose a 400 µm height for the channel that allows the circulation of damaged and/or swelling worms. This chip design enabled also a quick, safe and easy introduction of the worm couples that reduces manipulation as much as possible, and thus the risk of worm damage.

The flow rates generated in our system were simulated using a volumic mass of 1007 kg m^{-3} and a dynamic viscosity of 0.958 mPa s for the culture medium [42]. Electronic supplementary material, table S3 gives the values of the wall shear stress (WSS) (Pa), maximum velocity (m s^{-1}), Reynolds number and pressure gradient (Pa m^{-1}) obtained for different flow rates. The flow was found to be laminar (low Reynolds number) and the range of WSS ranged between 0.003 and 0.206 Pa (figure 3*b*; electronic supplementary material, figure S6). Thus, the range of flow rates used in our system reproduces the WSS conditions encountered by worms in the human blood system and in particular in veins and venules [43].

Finally, we showed that under dynamic conditions, fresh worms firmly attach to the walls, with a strong preference for the glass surface, and actively resist the flow (figure 3*c*). It is worth noting that most worm couples stayed paired, which is a sign of health, and that both males and females contributed to the attachment through their suckers. Immediately after starting and increasing the flow, damaged and/or weak worms were eliminated in a few minutes from the chip (10 to 15%) and were flushed out and pushed inside the outlet tubing, whereas healthy worms remained firmly gripped to the chip walls for hours.

3.2. Optimization of worm storage in *ex vivo* conditions

One of the major limiting factors to performing studies on adult schistosomes is their short survival period in basic culture media after perfusion from their vertebrate host. Since a continuous perfusion of 'fresh worms' is not ethically or practically feasible, proper storage of a sufficient worm population for several days is a critical element to compare successive experiments. Consequently, the culture of worms in an optimal medium is a key point for reliable experiments. Although several studies have aimed at identifying positive and negative factors contained in various sera [12,44–46] for worm culture, no firm conclusions regarding the most appropriate serum to use in our experiments could be drawn from previous reports. Therefore, and before starting the microfluidic experiments, we characterized different

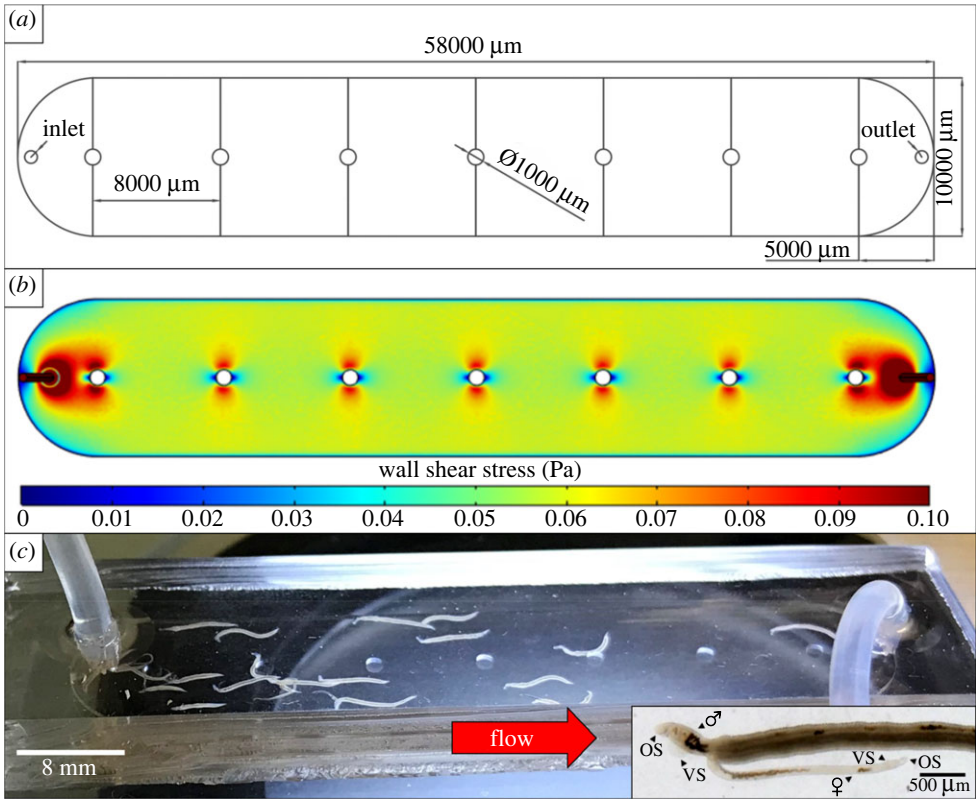

Figure 3. Microfluidic chip model. (*a*) Layout of the microfluidic device. Chamber of 58 000 µm of length, 10 000 µm of width, 400 µm of height and a pillar of 1000 µm of diameter every 8000 µm. Media input (Inlet) and output (Outlet) ports location; (*b*) numerical simulation of the WSS (colour gradient in Pa); (*c*) couples of schistosomes under flow conditions loaded in a collagen-coated chip (1 mL min^{-1}). Insert: Males (♂) and females (♀) attached to chip surface using their oral sucker (OS) and ventral sucker (VS).

media to identify those enabling the maintenance of the adult worms in a healthy status for at least 72 h after recovery from infected hamsters. We varied the cell culture basal medium (M199, DMEM and RPMI) and the serum additive (10% of heat-inactivated fetal calf, horse or human serum). Figure 4 shows the worm viability as a function of time for the different serum additives added to RPMI (see electronic supplementary material, figure S3 for M199 and DMEM). As expected, these data confirm that the absence of serum has a major impact on worm longevity with the entire population dead within 15 days. Worms maintained with human and horse serum showed a survival rate greater than 90% whatever the medium composition with no significant differences except when combined with M199 medium, which gave less than 90% of survival after 25 days of culture. Beyond this period, the viability of couples dropped drastically for all the culture media tested with; however, there was a better result for the RPMI and DMEM media. Surprisingly, calf serum, which is classically used for schistosome cultures, showed a significantly lower survival rate (70% at 29 days) with RPMI and even less for the other culture media tested (electronic supplementary material, figure S3b,c). Consequently, and even if our experiment was conducted shortly after worm recovery, we selected the combination of RPMI medium and horse serum for subsequent experiments. In addition, since serum performances can strongly vary from batch to batch, all experiments have been conducted with the same serum batches. Note that horse serum has the advantage of being easily accessible and safer to use than human serum.

3.3. Worm adhesion capabilities in microfluidic chips

The ability of the worm couples to grip the walls of the microfluidic system potentially depends on its geometry but also on the physico-chemical nature of the walls constituting the perfusion channel. Indeed, *in vivo*, adult worms mostly attach to the vein endothelium using their oral and ventral suckers together with a peristaltic action of the tegument [36]. In our system, without a confined geometry like that of veins, we logically observed that the attachment mostly relied on the ability of suckers to grip the chip surface (see electronic supplementary material, movies S1 and S2). This led us

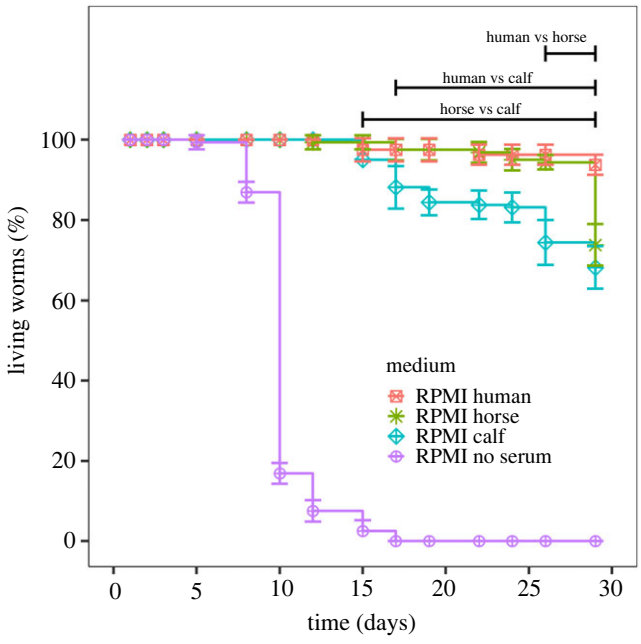

Figure 4. Progression of the survival rate of *S. mansoni* pairs as a function of time for RPMI culture media supplemented or not with human, calf or horse sera in static Petri dish culture conditions. Plot represents average of percentage of worm survival +/− standard error (10 couples, $n = 8$). Black bars indicate areas of statistical significance between sera after ANOVA (p-value < 0.05).

to examine the influence of different surface coatings on the resistance of the worms to the flow through the measurement of their residence time in the device.

We chose the MDCK cell line as the most effective cell coating because they are easy to grow and build a single cell layer strongly attaching to the raw glass surface. In addition, these cells quickly reach confluence in 48–72 h in a medium allowing the best viability of the worms (RPMI supplemented with horse sera). Figure 5*a* gives the percentage of worm couples in the chip as a function of the flow rate for the different coatings (raw glass, collagen, MDCK cells or MDCK cells on collagen). The responses of the worms to the flow showed a biphasic behaviour. A first linear response with a negative slope was immediately observed for the raw glass, glass + MDCK and collagen + MDCK-coated chips, with a transition value of the slopes occurring at approximately 1.6 mL min^{-1} (see electronic supplementary material, figures S4 and S5, table S2). By contrast, the collagen-coated chip was characterized by an initial plateau at 100% residence of worm pairs from 0 to 0.4 mL min^{-1} flow rate, followed by a linear response to the flow with a negative slope. The slope of the segment is a quantification of the resistance of the worms to the flow. For glass and glass + MDCK-coated surface, the loss of worms (56% and 57% loss per mL min^{-1}) is much larger than those occurring with the collagen and collagen + MDCK surfaces (38% and 22% loss per mL min^{-1}), and the difference of attachment capabilities between these two groups of conditions (i.e. with or without collagen) is significant from 0.7 to 2.8 mL min^{-1}. The initial plateau for the collagen chip suggests an easier initial gripping of the worms when the flow starts and increases. We tried to understand why such a difference exists in the worm gripping between the uncoated and the collagen-coated chips, independently of a cell layer. Close examination of the chips under the microscope revealed that worms firmly gripped the cell layer. However, after starting the flow, on the chips not coated with collagen, the cell layer 'pilled off' under sucker traction and worms were unable to reattach. Surprisingly, this phenomenon of cell detachment upon sucker traction was also observed on the collagen + MDCK-coated chips, making the cell layer heterogeneous and probably explaining the higher standard deviation in the dataset compared with the simple collagen-coating chips. Therefore, and counterintuitively, these data show that a simple collagen coating on a glass surface is sufficient to promote robust worm gripping by their suckers, whereas a cellular coating does not favour robust gripping and rather adds complexity and no advantage.

Since morphologies and gripping capabilities of worms are very different between males and females, we next compared the attachment of males, females and couples within the chip onto a collagen surfacing under increasing flow rate (figure 5*b*). Interestingly, males, females and couples

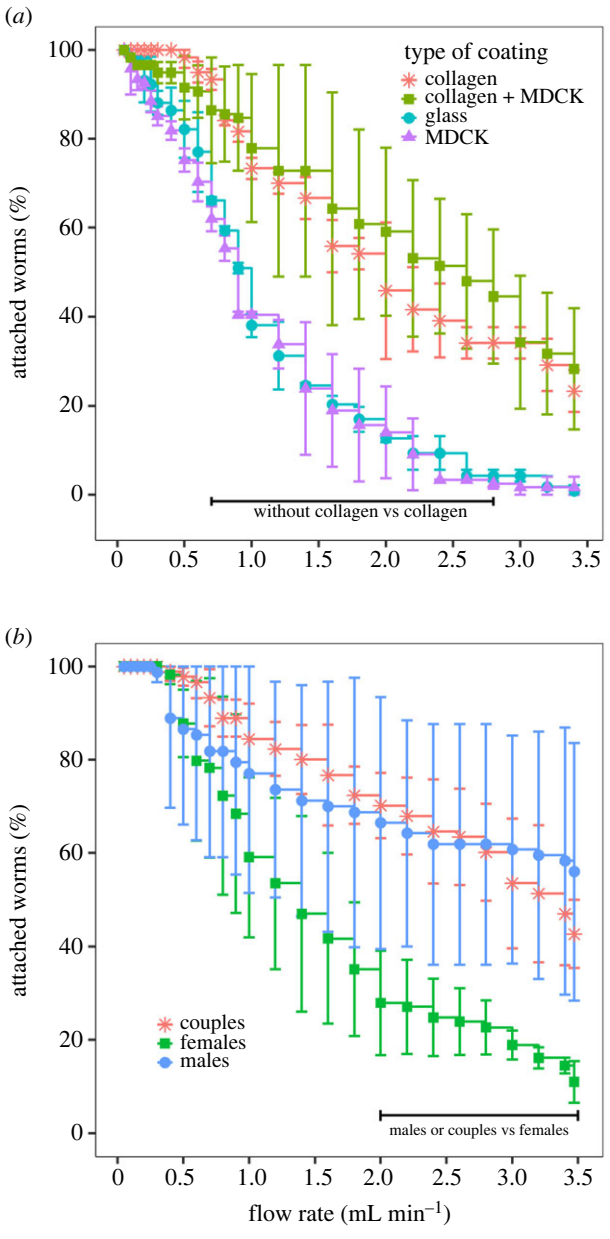

Figure 5. Worm attachment capabilities in microfluidic chip as a function of coatings and pairing status. (*a*) Evolution of schistosome couple attachment in the microfluidic chip as a function of flow rate for different internal wall coatings: none, collagen, MDCK cells and MDCK cells + collagen. Plot represents the average of percentage of worm attached +/− standard error (30 couples, $n = 3$). Black bar indicates the area of significance between coating types after ANOVA (p-value < 0.05). (*b*) Evolution of schistosome male, female or couple attachment in the microfluidic chip as a function of flow rate for different internal wall coatings: none, collagen, MDCK cells and MDCK cells + collagen. Plot represents average of percentage of worm attached +/− standard error (30 couples, $n = 3$). Black bar indicates area of statistical significance between coating types (collagen or collagen + MDCK versus glass or MDCK) after ANOVA (p-value < 0.05).

displayed a similar adhesion for flow rates under 2 mL min^{-1}. Above 2 mL min^{-1}, a significant attachment difference was observed between males and females as well as between females and couples, but not between males and couples. This observation confirms that surface gripping to chip mostly rely on males within worm couples. A difference in attachment between males and couples was only observed at very high flow rates, i.e. above 3 mL min^{-1}.

For the rest of this study, we thus selected a collagen surfacing which is easier to implement and gives robust and reproducible worm gripping at a flow rate of 1 mL min^{-1}. This flow rate allowed a greater than 80% couples retention but still forced firm gripping from the worms and allowed elimination of weak worms, primarily males, within a few minutes.

3.4. Determination of early effects by drugs in microfluidic device

Having defined the most reliable surface coating and flow rate for promoting worm residence in the microfluidic channels, we measured the effect of two well-known therapeutic molecules, PZQ and ART, on the ability of worms to grip to the chip surface under dynamic conditions. For these experiments, the microchannels were infused at a flow rate of 1 mL min^{-1} and the number of worms remaining in the microchannel was measured as a function of time for different doses of PZQ or ART (figure 6*a*,*b*,*f*,*g*).

We observed that a PZQ dose of 25 nM had no significant effect on worm gripping compared with the control (approximately 8% of the initial worm number were flushed out after 5 min and 30% after 50 min). The effect of PZQ started to be observed at 37.5 nM with 60% of the worms remaining in the system after 50 min (electronic supplementary material, movie S3 and figure S7). At 50 nM, we began to perceive erratic contractions of the worms and 50% of the worms were able to resist the flow after 50 min. From 100 to 400 nM, a rapid paralysis and thus detachment of the worms was observed, together with a significant swelling and a reduction in their length. Consequently, only 20% of the worms still remained after 10 min, while they were all carried away by the flow after 50 min. The IC_{50} values for 20, 30 and 50 min residence times are reported in table 1. Importantly, we noticed that after 20 min of treatment, IC_{50} values were similar and close to 60 nM, suggesting that the effect of the drug on the worms is optimal after 20 min and up to 50 min of perfusion, but this can still be extended if needed.

Next, we evaluated the effect of ART on worm gripping under microfluidic conditions. Worms started to detach from the chip at a dose of 50 µM (figure 6*f*,*g*). At this concentration, 62% of the worms remained attached after 50 min (electronic supplementary material, movie S8 and figure S8). Above 75 µM, the effect of the drug on worm morphology began to be noticeable and led to a massive flush-out (7% attached). Again, the calculated IC_{50} values at 20, 30 and 50 min were almost identical at 58 µM.

In parallel and using the same batch of worms (i.e. from the same perfusion and culture duration), we also determined IC_{50} values for PZQ or ART using the classical method in Petri dishes under static conditions. We observed a very sharp effect of PZQ since after 120 h a dramatic change in the scoring occurred between 150 and 300 nM (electronic supplementary material, movies S4–S7), leading to an IC_{50} value of 245 nM.

The effect of ART on worm viability was much more gradual. Worms started to degrade and to die from 12.5 up to 400 µM, where all worms were classified as dead (electronic supplementary material, movies S9–S12). This resulted in an IC_{50} value of 200 µM after 120 h of exposure to ART. Since these experiments in static conditions lasted 120 h and to ensure that our IC_{50} measurements were not influenced by medium composition, we also determined the IC_{50} in M199 with calf serum. The values obtained were almost identical and the corresponding IC_{50} values for PZQ and ART from these Petri dish experiments are collected in table 2.

Even if the measured phenotypes (attachment versus survival) are different and thus difficult to compare side by side, the IC_{50} values obtained in dynamic conditions are in the same range as those obtained in 'classical' static condition for PZQ and ART. This suggests that our microfluidic device allows anticipation of drug effects in less than 20 min.

4. Discussion

The identification of new drugs to treat schistosomiasis is one of the priorities of WHO for parasite control [47]. Despite decades of research to identify an alternative to PZQ, this molecule remains the only one recommended to treat this parasitosis [12]. The mode of action of PZQ has been recently elucidated [48] more than 40 years after the observation of its antihelmintic activity [49]. PZQ acts on the transient receptor potential channel (TRPM), whose activation instantaneously paralyses worms. *In vivo*, PZQ leads to worm death by altering their surface tegument and giving access to the immune system. Therefore, the design of PZQ derivatives, possibly more potent and specific for the schistosome, is ongoing [50] together with the identification of a specific acquired resistance by mutation of the TRPM target [27]. However, the identification of new drugs remains highly limited by the limited number of assays dedicated to adult schistosomes [13]. Drug selection still remains dependent on the observation of complex phenotypes and/or sophisticated image analysis of worm motility, egg laying or pairing [20]. In addition, the altered viability of adult worms in *in vitro* culture

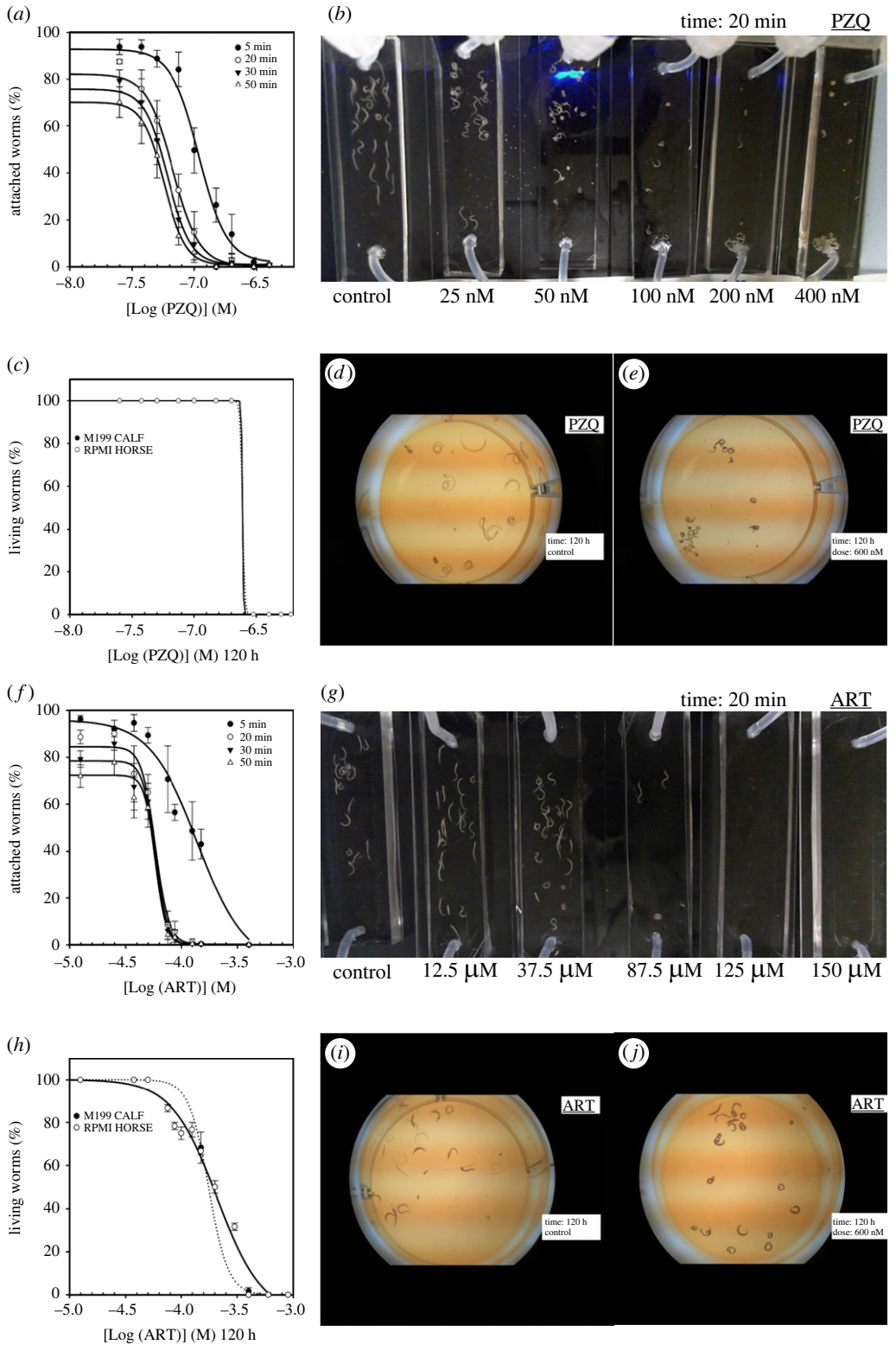

Figure 6. Microfluidic and static IC_{50} determinations of responses to PZQ and ART. (*a*) Microfluidic determination of IC_{50} based on percentage of schistosomes attached to collagen chip surface at 5, 20, 30 and 50 min depending on PZQ doses; (*b*) representative image of six chip series at 20 min using six doses of PZQ (control, 25, 50, 100, 200 and 400 nM) with 30 couples per chip at 1 mL min^{-1} flow rate; (*c*) static determination of IC_{50} based on percentage of living schistosomes at 120 h depending on PZQ doses; (*d*) representative image of one well of a PZQ negative control at 120 h with 10 couples; (*e*) representative image of one well with a 600 nM PZQ dose at 120 h with 10 worm couples; (*f*) microfluidic determination of IC_{50} based on percentage of schistosomes attached to collagen chip surface at 5, 20, 30 and 50 min depending on ART doses; (*g*) representative image of six chip series at 20 min using six doses of ART (control, 25, 50, 100, 200 and 400 nM) with 30 couples per chip at 1 mL min^{-1} flow rate; (*h*) static determination of IC_{50} based on percentage of schistosomes at 120 h depending on ART doses; (*i*) representative image of one well of an ART negative control at 120 h with 10 couples; (*j*) representative image of one well with a 600 nM ART dose at 120 h with 10 couples.

Table 1. Residence IC_{50} values determined in dynamic conditions. These values correspond to the concentration of PZQ or ART that induced 50% of worm detachment from the collagen-coated chips after 5, 20, 30 or 50 min of treatment at a flow rate of 1 mL min^{-1} in RPMI horse medium. Data are presented with their 95% confidence intervals (CI).

	PZQ	ART
time (min)	$IC_{50} \pm 95\%$ CI (nM)	$IC_{50} \pm 95\%$ CI (µM)
5	109 ± 13	139 ± 42
20	67 ± 10	58 ± 5
30	61 ± 9	58 ± 5
50	57 ± 7	58 ± 6

Table 2. Worm death IC_{50} values determined in static conditions. These values correspond to the concentration of PZQ or ART that induced 50% of worm death using a five-level severity score in six-well Petri dish format after 120 h of treatment in RPMI horse and M199 calf medium. Data are presented with their 95% CI.

	PZQ (120 h)	ART (120 h)
medium/serum	$IC_{50} \pm 95\%$ CI (nM)	$IC_{50} \pm 95\%$ CI (µM)
RPMI/horse	245 ± 5	176 ± 30
M199/calf	245 ± 1	208 ± 24

systems and the rapid loss of their biological functions can bias the results, particularly in the case of slow-acting compounds or not immediately acting on glucose metabolism such as PZQ [27] and not detectable in some metabolic assays [24]. Selection and functional characterization of active compounds on whole worms, i.e. a multicellular organism, are thus still a challenge since they require a comprehensive screen including motility and vitality but also pairing stability, egg production, surface flexibility/stiffness, attachment capacity and morphological changes over a sufficient time frame.

Monitoring the state of a living cell assembly at the level of a single cell, tissue, organ or whole body is carried out by quantifying various parameters usually identified by fluorescent or radiolabelled markers. These techniques are often destructive for the sample and performed at the end of the experiment. Label-free and real-time techniques have developed significantly for several years [35] and, in particular, applied in the field of organ-on-a-chip [51]. Impedance spectroscopy is such a label-free technique suitable for quantifying the properties of cell assemblies in real time [52]. It is compatible with high-throughput analyses and allows kinetics of the biological process to be measured and studied.

However, given the complexity of a cell assembly in a living worm, the interpretation of electrical data and the link to biological processes remain difficult to disentangle in many configurations. These methods are under development for monitoring schistosomula viability [53]. Their parallelization should provide an effective tool for the screening of drug libraries [51,53]. Despite these new technological advances, application to older worm stages (juvenile and adults) and particularly paired couples is very unlikely due to their large size (approx. 1 cm).

The study of whole animals in a smart microfluidic system is a very recent research topic in the field of systems biology. Some basic systems have been reported for the study of the free-living *Caenorhabditis elegans* worm [54,55]. By contrast, studies on trematodes are scare and mostly focused on worm locomotion mechanistics [36]. In parallel, progress has been made on the use of microfluidics for the detection of the parasites in human fluid either by microfluidic PCR, antigen identification or egg isolation [56]. The application of microfluidic technologies to the study of adult worm couple viability and fertility, or the evaluation of drug effects remains to be explored.

One significant limitation for adapting these microsystems to the study of adult worms is the limited optimal viability of adult worms '*ex vivo*'. Therefore, the analysis of long-lasting effects of drugs can be

difficult to distinguish from the natural degradation of worms outside their host. Recently, major advances have been done in the improvement of juvenile and adult worm culture media [12,35]. These optimized media allow the *in vitro* maintenance of fertile worms for a few weeks. Their efficacy was assessed in using mobility and pairing together with female reproductive organ development and sustained egg production as the main criteria of effectiveness. Even if the *in vitro* production of mature eggs (less than 10% of total eggs) generating infective miracidia is frequently observed in the schistosome community and was once formally described [57], surprisingly these media optimizations did not improved the hatching rate and the infectiveness, suggesting that medium optimization is not the only parameter to take into consideration for long-term maintenance of fertile parasites *ex vivo* [35]. Therefore, we have chosen to design a fluidic system that allows a quick measurement of a single and basic phenotypic parameter characteristic of healthy parasites: the surface attachment by suckers. This system necessarily selects healthy worms (males, females or couples) since it promotes the worm muscular reflex to attach onto the surface in a dynamic environment mimicking the blood flows occurring *in vivo*. In the portal system and in particular in the mesenteric vein where parasites reside, the flow speed is about $0.001\ \mathrm{m\ s^{-1}}$ and WSS estimated to be around 0.3 Pa [43,58]. Reproduction of these flow conditions is absolutely necessary to ensure that the worms are under realistic mechanical stress conditions that make the test more predictive and avoid over- or under-estimation of the effect of molecules on the adhesion capacity of worms. In particular, we showed that a simple collagen coating strongly improves the ability of worms to firmly grip with their suckers onto the glass surface even at high flow rates. A recent study demonstrates that worm attachment and crawling into vessels is a very sophisticated process based on a precise sucker's coordination [36]. While this parameter cannot be considered in static systems, it is an easy and powerful indicator of worm health and viability that has been overlooked. A major technical advantage of our system is that it does not require long-lasting image analysis since scoring is based on a binary method of evaluation: attached or not.

We chose to validate our system using the two major drugs used against the parasite, PZQ and ART. These compounds have different modes of action. PZQ triggers a sudden calcium efflux that paralyses worms and thus has an immediate effect on worm attachment capability. By contrast, the mode of action of ART is more pleiotropic with the production of free radicals that requires the presence of heme in the worm gut, a by-product of haemoglobin degradation [59]. The production of free radicals induces both oxidative and metabolic stresses and results in damage to tegument, tissues and reproductive organs [60,61]. Thus, contrary to PZQ, ART was not expected to promote an immediate effect on worms. Surprisingly, we observed a quick effect on worm attachment in a time- and concentration-dependent manner for both compounds. Moreover, we obtained IC_{50} values under flow conditions that are significantly lower than those measured under static conditions. For example, we obtained for PZQ an IC_{50} of 57 ± 7 nM at 50 min with the fluidic system compared with an IC_{50} of 245 ± 1 nM in the static system at 120 h. Similarly, ART gives an IC_{50} of 58 ± 6 µM in the device compared with an IC_{50} of 176 ± 30 µM in a Petri dish at 120 h in M199 calf serum. These results highlight the difficulty in comparing phenotypic assays performed under different conditions. Our microfluidic system must be considered as a novel phenotypic assay that is particularly sensitive due to the measurement of worm attachment capability.

One asset of the system described here is that it allows parallelization and simultaneous comparisons in using a larger number of live worms (30–40 couples) per condition compared with image-based or metabolic assays (5–10 couples), thus facilitating the reproducibility of experiments [13].

Evidently, our dynamic system does not pre-judge the delayed lethal effect of tested compounds but rather gives a direct insight into their toxicity and visualizes an immediate effect compared with long-term experiments in Petri dishes. Importantly, our study has been realized on worm couples as an initial proof of concept but these investigations can be extended to males and females alone in order to distinguish sex-specific effect of drugs but will need adjustment of flow parameters between separated sexes. Besides the sensitivity of worm gripping to drugs, other factors can contribute to the differences observed between flow and static conditions. Indeed, the flow rate has probably a major effect on drug distribution and metabolization compared with static conditions. Schistosomula and adult schistosomes have a very active metabolism characterized by a massive glucose consumption [62] associated with lactate production [63] and excretion [64]. However, high lactate production, which can be conveniently measured to assess worm active metabolism [28], and its accumulation due to a low diffusion rate in a static environment generates local acidification around worms. This acidification is well described to modify metabolization of drugs in cancer treatments [65]. Under flow conditions, the permanent actuation of drugs and culture medium probably reflects more the physiological conditions encountered by the worms in the bloodstream.

Finally, and conveniently, flushed-out worms can be retrieved from the devices, and further investigations such as metabolic or image analysis can be performed. In addition, the exchange of active compounds or pulse-chase treatment sequences can be easily performed in such a device. Finally, the entire device (chip and tubing) consumes an adjustable and reasonable amount of circulating fluid (as low as 1 mL) and thus minimizes the costs associated with the use of elaborate media and/or active molecules in a dynamic system.

Having established the proof of concept that our microsystem is reliable for the identification of active molecules against the parasite, we now aim to test further series of drugs together with the implementation of automated worm counting by simple real-time image analysis.

5. Conclusion

Selection and characterization of schistosomicidal drugs still remain major challenges and require relevant screening systems together with an improvement of the longevity of the parasite *in vitro*. Even if classical phenotypic screenings in Petri dishes can provide complementary information, they are mostly based on worm motion and/or tissue integrity. Therefore, the design of novel systems enabling a practical and rapid identification of molecules acting on the parasite is desirable. We report such a system that can be parallelized with a large number of worms per condition and relying on a simple phenotype, i.e. the attachment of worms to the chip surface under flow conditions. It is also affordable, can be automated and thus should facilitate the identification of new drugs against this re-emerging parasite.

Ethics. All animal experimentations were conducted in accordance with the European Convention for the Protection of Vertebrate Animals used for Experimental and other Scientific Purposes (ETS no. 123, revised Appendix A) and were approved by the local committee for ethics in animal experimentation (authorization no. APAFIS#8289-2016122015127050v3) and the Pasteur Institute of Lille (agreement no. B59350009).

Data accessibility. All data files are provided as movies and tables in the electronic supplementary material [66], and all raw source data (uncompressed videos, Rstudio scripts, codes, simulations files) have been uploaded on Dryad Digital Repository: https://doi.org/10.5061/dryad.qv9s4mwhc [67].

Authors' contributions. V.G.: conceptualization, data curation, formal analysis, methodology and writing—original draft; R.H.: data curation, methodology and visualization; K.S.: conceptualization, data curation, formal analysis, methodology, supervision, validation and writing—review and editing; M.-J.G.: methodology and supervision; S.C.: methodology, project administration and supervision; O.M.: funding acquisition, investigation, methodology, resources, supervision and writing—review and editing; C.D.: conceptualization, supervision and writing—review and editing; V.S.: conceptualization, formal analysis, funding acquisition, investigation, methodology, project administration, resources, supervision, validation, visualization and writing—review and editing; J.V.: conceptualization, formal analysis, funding acquisition, investigation, methodology, project administration, resources, supervision, validation, visualization and writing—review and editing.

All authors gave final approval for publication and agreed to be held accountable for the work performed therein.

Conflict of interest declaration. The authors declare no conflict of interest. The funders had no role in the design of the study; in the collection, analyses, or interpretation of data; in the writing of the manuscript, or in the decision to publish the results.

Funding. This research was funded in part by the french National Research Agency (ANR) under project ANR-21-CE19-0049-02, by CPER-CTRL program from Region Hauts-de-France (ChipsToSoma Exploratory project), by I-SITE program from University of Lille (SnowMan Expand project) and by CNRS recurring endowment to UMR9017.

Acknowledgements. We thank Dr Raymond Pierce for helpful discussions and paper proof reading, and members of the PLEHTA (Institut Pasteur de Lille Animal Facility) for high quality technical support. We thank Dr Jean-Claude Gerbedoen (LIMMS) for technical support in clean-room operations.

References

1. WHO. 2022 *Schistosomiasis*. See https://www.who.int/news-room/fact-sheets/detail/schistosomiasis.
2. Colley DG, Bustinduy AL, Secor WE, King CH. 2014 Human schistosomiasis. *Lancet* **383**, 2253–2264. (doi:10.1016/S0140-6736(13)61949-2)
3. Boissier J *et al.* 2016 Outbreak of urogenital schistosomiasis in Corsica (France): an epidemiological case study. *Lancet Infect. Dis.* **16**, 971–979. (doi:10.1016/S1473-3099(16)00175-4)
4. Nation CS, Da'dara AA, Marchant JK, Skelly PJ. 2020 Schistosome migration in the definitive host. *PLoS Negl. Trop. Dis.* **14**, e0007951. (doi:10.1371/journal.pntd.0007951)
5. Molehin AJ. 2020 Schistosomiasis vaccine development: update on human clinical trials. *J. Biomed. Sci.* **27**, 28. (doi:10.1186/s12929-020-0621-y)

6. Mader P, Rennar GA, Ventura AMP, Grevelding CG, Schlitzer M. 2018 Chemotherapy for fighting schistosomiasis: past, present and future. *ChemMedChem* **13**, 2374–2389. (doi:10.1002/cmdc.201800572)
7. Secor WE, Montgomery SP. 2015 Something old, something new: is praziquantel enough for schistosomiasis control? *Future Med. Chem.* **7**, 681–684. (doi:10.4155/fmc.15.9)
8. Wang W, Wang L, Liang YS. 2012 Susceptibility or resistance of praziquantel in human schistosomiasis: a review. *Parasitol. Res.* **111**, 1871–1877. (doi:10.1007/s00436-012-3151-z)
9. Melman SD *et al.* 2009 Reduced susceptibility to praziquantel among naturally occurring Kenyan isolates of *Schistosoma mansoni*. *PLoS Negl. Trop. Dis.* **3**, e504. (doi:10.1371/journal.pntd.0000504)
10. Fallon PG, Doenhoff MJ. 1994 Drug-resistant schistosomiasis: resistance to praziquantel and oxamniquine induced in *Schistosoma mansoni* in mice is drug specific. *Am. J. Trop. Med. Hyg.* **51**, 83–88. (doi:10.4269/ajtmh.1994.51.83)
11. Crellen T, Walker M, Lamberton PH, Kabatereine NB, Tukahebwa EM, Cotton JA, Webster JP. 2016 Reduced efficacy of praziquantel against *Schistosoma mansoni* is associated with multiple rounds of mass drug administration. *Clin. Infect. Dis.* **63**, 1151–1159. (doi:10.1093/cid/ciw506)
12. Buchter V, Schneeberger PHH, Keiser J. 2021 Validation of a human-serum-based *in vitro* growth method for drug screening on juvenile development stages of *Schistosoma mansoni*. *PLoS Negl. Trop. Dis.* **15**, e0009313. (doi:10.1371/journal.pntd.0009313)
13. Moreira-Filho JT *et al.* 2021 Schistosomiasis drug discovery in the era of automation and artificial intelligence. *Front. Immunol.* **12**, 642383. (doi:10.3389/fimmu.2021.642383)
14. Paveley RA *et al.* 2012 Whole organism high-content screening by label-free, image-based Bayesian classification for parasitic diseases. *PLoS Negl. Trop. Dis.* **6**, e1762. (doi:10.1371/journal.pntd.0001762)
15. Chen S, Suzuki BM, Dohrmann J, Singh R, Arkin MR, Caffrey CR. 2020 A multi-dimensional, time-lapse, high content screening platform applied to schistosomiasis drug discovery. *Commun. Biol.* **3**, 747. (doi:10.1038/s42003-020-01402-5)
16. Mansour NR, Bickle QD. 2010 Comparison of microscopy and Alamar blue reduction in a larval based assay for schistosome drug screening. *PLoS Negl. Trop. Dis.* **4**, e795. (doi:10.1371/journal.pntd.0000795)
17. Lalli C, Guidi A, Gennari N, Altamura S, Bresciani A, Ruberti G. 2015 Development and validation of a luminescence-based, medium-throughput assay for drug screening in *Schistosoma mansoni*. *PLoS Negl. Trop. Dis.* **9**, e0003484. (doi:10.1371/journal.pntd.0003484)
18. Ravaynia PS, Lombardo FC, Biendl S, Dupuch MA, Keiser J, Hierlemann A, Modena MM. 2020 Parallelized impedance-based platform for continuous dose-response characterization of antischistosomal drugs. *Adv. Biosyst.* **4**, e1900304. (doi:10.1002/adbi.201900304)
19. Ravaynia PS, Biendl S, Grassi F, Keiser J, Hierlemann A, Modena MM. 2022 Real-time and automated monitoring of antischistosomal drug activity profiles for screening of compound libraries. *iScience* **25**, 104087. (doi:10.1016/j.isci.2022.104087)
20. Ramirez B, Bickle Q, Yousif F, Fakorede F, Mouries MA, Nwaka S. 2007 Schistosomes: challenges in compound screening. *Expert Opin. Drug Discov.* **2**(s1), S53–S61. (doi:10.1517/17460441.2.S1.S53)
21. Neves BJ *et al.* 2016 Discovery of new anti-schistosomal hits by integration of QSAR-based virtual screening and high content screening. *J. Med. Chem.* **59**, 7075–7088. (doi:10.1021/acs.jmedchem.5b02038)
22. Rinaldi G, Loukas A, Brindley PJ, Irelan JT, Smout MJ. 2015 Viability of developmental stages of *Schistosoma mansoni* quantified with xCELLigence worm real-time motility assay (xWORM). *Int. J. Parasitol. Drugs Drug Resist.* **5**, 141–148. (doi:10.1016/j.ijpddr.2015.07.002)
23. Manneck T, Braissant O, Haggenmuller Y, Keiser J. 2011 Isothermal microcalorimetry to study drugs against *Schistosoma mansoni*. *J. Clin. Microbiol.* **49**, 1217–1225. (doi:10.1128/JCM.02382-10)
24. Aguiar PHN, Fernandes N, Zani CL, Mourao MM. 2017 A high-throughput colorimetric assay for detection of *Schistosoma mansoni* viability based on the tetrazolium salt XTT. *Parasit. Vectors* **10**, 300. (doi:10.1186/s13071-017-2240-3)
25. Wang J *et al.* 2015 Intake of erythrocytes required for reproductive development of female *Schistosoma japonicum*. *PLoS ONE* **10**, e0126822. (doi:10.1371/journal.pone.0126822)
26. Galanti SE, Huang SC, Pearce EJ. 2012 Cell death and reproductive regression in female *Schistosoma mansoni*. *PLoS Negl. Trop. Dis.* **6**, e1509. (doi:10.1371/journal.pntd.0001509)
27. Le Clec'h W *et al.* 2021 Genetic analysis of praziquantel response in schistosome parasites implicates a transient receptor potential channel. *Sci. Transl. Med.* **13**, eabj9114. (doi:10.1126/scitranslmed.abj9114)
28. Howe S, Zophel D, Subbaraman H, Unger C, Held J, Engleitner T, Hoffmann WH, Kreidenweiss A. 2015 Lactate as a novel quantitative measure of viability in *Schistosoma mansoni* drug sensitivity assays. *Antimicrob. Agents Chemother.* **59**, 1193–1199. (doi:10.1128/AAC.03809-14)
29. Geary TG, Sakanari JA, Caffrey CR. 2015 Anthelmintic drug discovery: into the future. *J. Parasitol.* **101**, 125–133. (doi:10.1645/14-703.1)
30. Aulner N, Danckaert A, Ihm J, Shum D, Shorte SL. 2019 Next-generation phenotypic screening in early drug discovery for infectious diseases. *Trends Parasitol.* **35**, 559–570. (doi:10.1016/j.pt.2019.05.004)
31. Marcellino C, Gut J, Lim KC, Singh R, McKerrow J, Sakanari J. 2012 WormAssay: a novel computer application for whole-plate motion-based screening of macroscopic parasites. *PLoS Negl. Trop. Dis.* **6**, e1494. (doi:10.1371/journal.pntd.0001494)
32. Gardner JMF, Mansour NR, Bell AS, Helmby H, Bickle Q. 2021 The discovery of a novel series of compounds with single-dose efficacy against juvenile and adult *Schistosoma* species. *PLoS Negl. Trop. Dis.* **15**, e0009490. (doi:10.1371/journal.pntd.0009490)
33. Lombardo FC, Pasche V, Panic G, Endriss Y, Keiser J. 2019 Life cycle maintenance and drug-sensitivity assays for early drug discovery in *Schistosoma mansoni*. *Nat. Protoc.* **14**, 461–481. (doi:10.1038/s41596-018-0101-y)
34. Padalino G, Ferla S, Brancale A, Chalmers IW, Hoffmann KF. 2018 Combining bioinformatics, cheminformatics, functional genomics and whole organism approaches for identifying epigenetic drug targets in *Schistosoma mansoni*. *Int. J. Parasitol. Drugs Drug Resist.* **8**, 559–570. (doi:10.1016/j.ijpddr.2018.10.005)
35. Wang J, Chen R, Collins III JJ. 2019 Systematically improved in vitro culture conditions reveal new insights into the reproductive biology of the human parasite *Schistosoma mansoni*. *PLoS Biol.* **17**, e3000254. (doi:10.1371/journal.pbio.3000254)
36. Zhang S, Skinner D, Joshi P, Criado-Hidalgo E, Yeh YT, Lasheras JC, Caffrey CR, Del Alamo JC. 2019 Quantifying the mechanics of locomotion of the schistosome pathogen with respect to changes in its physical environment. *J. R. Soc. Interface* **16**, 20180675. (doi:10.1098/rsif.2018.0675)
37. Smithers SR, Terry RJ. 1965 Acquired resistance to experimental infections of *Schistosoma mansoni* in the albino rat. *Parasitology* **55**, 711–717. (doi:10.1017/S0031182000086261)
38. Xiao S, Chollet J, Utzinger J, Matile H, Mei J, Tanner M. 2001 Artemether administered together with haemin damages schistosomes *in vitro*. *Trans. R. Soc. Trop. Med. Hyg.* **95**, 67–71. (doi:10.1016/S0035-9203(01)90336-0)
39. Abdulla MH *et al.* 2009 Drug discovery for schistosomiasis: hit and lead compounds identified in a library of known drugs by medium-throughput phenotypic screening. *PLoS Negl. Trop. Dis.* **3**, e478. (doi:10.1371/journal.pntd.0000478)
40. R Core Team. 2022 *R: a language and environment for statistical computing*. Vienna, Austria: R Foundation for Statistical Computing. See https://www.R-project.org/.
41. Heyries KA, Hansen CL. 2011 Parylene C coating for high-performance replica molding. *Lab. Chip* **11**, 4122–4125. (doi:10.1039/c1lc20623k)
42. Poon C. 2022 Measuring the density and viscosity of culture media for optimized computational fluid dynamics analysis of *in vitro* devices. *J. Mech. Behav. Biomed. Mater.* **126**, 105024. (doi:10.1016/j.jmbbm.2021.105024)
43. Papaioannou TG, Stefanadis C. 2005 Vascular wall shear stress: basic principles and methods. *Hellenic J. Cardiol.* **46**, 9–15.
44. Clegg JA. 1965 *In vitro* cultivation of *Schistosoma Mansoni*. *Exp. Parasitol.* **16**, 133–147. (doi:10.1016/0014-4894(65)90037-8)
45. Basch PF. 1981 Cultivation of *Schistosoma mansoni* in vitro. II. Production of infertile eggs by worm pairs cultured from cercariae. *J. Parasitol.* **67**, 186–190. (doi:10.2307/3280633)
46. Anisuzzaman FS, Prodjinotho UF, Bhattacharjee S, Verschoor A, da Costa C P. 2021 Host-specific serum factors control the development and

survival of *Schistosoma mansoni*. *Front. Immunol.* **12**, 635622. (doi:10.3389/fimmu.2021.635622)

47. Siqueira LDP *et al.* 2017 Schistosomiasis: drugs used and treatment strategies. *Acta Trop.* **176**, 179–187. (doi:10.1016/j.actatropica.2017.08.002)
48. Park SK, Gunaratne GS, Chulkov EG, Moehring F, McCusker P, Dosa PI, Chan JD, Stucky CL. 2019 The anthelmintic drug praziquantel activates a schistosome transient receptor potential channel. *J. Biol. Chem.* **294**, 18 873–18 880. (doi:10.1074/jbc.AC119.011093)
49. Cioli D, Pica-Mattoccia L. 2003 Praziquantel. *Parasitol. Res.* **90**(Supp 1), S3–S9. (doi:10.1007/s00436-002-0751-z)
50. Park SK, Marchant JS. 2020 The journey to discovering a flatworm target of praziquantel: a long TRP. *Trends Parasitol.* **36**, 182–194. (doi:10.1016/j.pt.2019.11.002)
51. Modena M, Chawla K, Lombardo F, Bürgel S, Panic G, Keiser J, Hierlemann A. 2017 Impedance-based detection of *Schistosoma mansoni* larvae viability for drug screening. In *IEEE Xplore. Biomedical Circuits and Systems Conference (BioCAS)*. (doi:10.1109/BIOCAS.2017.8325227)
52. Marxer M, Ingram K, Keiser J. 2012 Development of an *in vitro* drug screening assay using *Schistosoma haematobium schistosomula*. *Parasit. Vectors* **5**, 165. (doi:10.1186/1756-3305-5-165)
53. Nacif-Pimenta R *et al.* 2019 Differential responses of epithelial cells from urinary and biliary tract to eggs of *Schistosoma haematobium* and *S. mansoni*. *Sci. Rep.* **9**, 10731. (doi:10.1038/s41598-019-46917-y)
54. Weeks JC, Roberts WM, Robinson KJ, Keaney M, Vermeire JJ, Urban Jr JF, Lockery SR, Hawdon JM. 2016 Microfluidic platform for electrophysiological recordings from host-stage hookworm and *Ascaris suum* larvae: a new tool for anthelmintic research. *Int. J. Parasitol. Drugs Drug Resist.* **6**, 314–328. (doi:10.1016/j.ijpddr.2016.08.001)
55. Gokce SK, Hegarty EM, Mondal S, Zhao P, Ghorashian N, Hilliard MA, Ben-Yakar A. 2017 A multi-trap microfluidic chip enabling longitudinal studies of nerve regeneration in *Caenorhabditis elegans*. *Sci. Rep.* **7**, 9837. (doi:10.1038/s41598-017-10302-4)
56. Nigo MM, Salieb-Beugelaar G, Battegay M, Odermatt P, Hunziker P. 2019 Schistosomiasis: from established diagnostic assays to emerging micro/nanotechnology-based rapid field testing for clinical management and epidemiology. *Precision Nanomed.* **3**, 439–458. (doi:10.33218/prnano3(1).191205.1)
57. Newport GR, Weller TH. 1982 Miracidia infective for snails derived from eggs laid by adult *Schistosoma mansoni in vitro*. *Parasitology* **84**, 481–490. (doi:10.1017/S0031182000052781)
58. Brown HS, Halliwell M, Qamar M, Read AE, Evans JM, Wells PN. 1989 Measurement of normal portal venous blood flow by Doppler ultrasound. *Gut* **30**, 503–509. (doi:10.1136/gut.30.4.503)
59. Sun J, Li C, Wang S. 2016 Organism-like formation of *Schistosoma hemozoin* and its function suggest a mechanism for anti-malarial action of artemisinin. *Sci. Rep.* **6**, 34463.
60. Sun J, Hu W, Li C. 2013 Beyond heme detoxification: a role for hemozoin in iron transport in *S. japonicum*. *Parasitol. Res.* **112**, 2983–2990. (doi:10.1007/s00436-013-3470-8)
61. Saeed MEM, Krishna S, Greten HJ, Kremsner PG, Efferth T. 2016 Antischistosomal activity of artemisinin derivatives *in vivo* and in patients. *Pharmacol. Res.* **110**, 216–226. (doi:10.1016/j.phrs.2016.02.017)
62. Bueding E. 1950 Carbohydrate metabolism of *Schistosoma mansoni*. *J. Gen. Physiol.* **33**, 475–495. (doi:10.1085/jgp.33.5.475)
63. Horemans AM, Tielens AG, van den Bergh SG. 1992 The reversible effect of glucose on the energy metabolism of *Schistosoma mansoni* cercariae and schistosomula. *Mol. Biochem. Parasitol.* **51**, 73–79. (doi:10.1016/0166-6851(92)90202-U)
64. Faghiri Z, Camargo SM, Huggel K, Forster IC, Ndegwa D, Verrey F, Skelly PJ. 2010 The tegument of the human parasitic worm *Schistosoma mansoni* as an excretory organ: the surface aquaporin SmAQP is a lactate transporter. *PLoS ONE* **5**, e10451. (doi:10.1371/journal.pone.0010451)
65. Mahoney BP, Raghunand N, Baggett B, Gillies RJ. 2003 Tumor acidity, ion trapping and chemotherapeutics. I. Acid pH affects the distribution of chemotherapeutic agents in vitro. *Biochem. Pharmacol.* **66**, 1207–1218. (doi:10.1016/S0006-2952(03)00467-2)
66. Girod V, Houssier R, Sahmer K, Ghoris M-J, Caby S, Melnyk O, Dissous C, Senez V, Vicogne J. 2022 A self-purifying microfluidic system for identifying drugs acting against adult schistosomes. Figshare. (doi:10.6084/m9.figshare.c.6306035)
67. Girod V, Houssier R, Sahmer K, Ghoris M-J, Caby S, Melnyk O, Dissous C, Senez V, Vicogne J. 2022 Data from: A self-purifying microfluidic system for identifying drugs acting against adult schistosomes. Dryad Digital Repository. (https://doi.org/10.5061/dryad.qv9s4mwhc)